Experiment vs simulation RT WFNDEC 2014 benchmark: CIVA results

D. Tisseur, M. Costin, B. Rattoni, C. Vienne, A. Vabre, G. Cattiaux[b], T. Sollier[b]

[a)] *CEA LIST, CEA Saclay 91191 Gif sur Yvette Cedex, France*
[b)] *Institut de Radioprotection et de Sûreté Nucléaire,B.P.17 92262 Fontenay-Aux-Roses, France*
[a)] Corresponding author: david.tisseur@cea.fr

Abstract. The French Atomic Energy Commission and Alternative Energies (CEA) has developed for years the CIVA software dedicated to simulation of NDE techniques such as Radiographic Testing (RT). RT modelling is achieved in CIVA using combination of a determinist approach based on ray tracing for transmission beam simulation and a Monte Carlo model for the scattered beam computation. Furthermore, CIVA includes various detectors models, in particular common x-ray films and a photostimulable phosphor plates. This communication presents the results obtained with the configurations proposed in the World Federation of NDEC 2014 RT modelling benchmark with the RT models implemented in the CIVA software.

INTRODUCTION

In the RT WFNDEC benchmarks of previous years the validation was performed through a code inter-comparison, without comparing experimental data. Since the detector modeling was excluded, the validation only took into account the photons at the detector entrance. This year a benchmark for RT code validation by comparison with experimental data has been proposed. This benchmark is the part of the WFNDEC 2014 benchmark. Two types of detectors are considered, namely X-ray films and image plates. The benchmark concerns:

2 gamma-ray sources: Se75 and Ir192
4 detectors:
* 2 films, high and low sensitivity (KODAK M100 and KODAK AA400 respectively)
* 2 image plates, fine and coarse grains (KODAK HR and KODAK GP respectively)

The experiments have been done at CEA and the experimental data are available on the WFNDEC website [1]. After a brief description of the experimental set-up we report the results obtained with CIVA.

BENCHMARK DESCRIPTION

The benchmark is based on a ferritic steel step wedge 272 mm long by 100 mm large composed of 7 steps (4, 6, 8, 10, 12, 15 and 18 mm). The first six steps are 40 mm long while the thickest step is 32 mm long (see fig. 1)

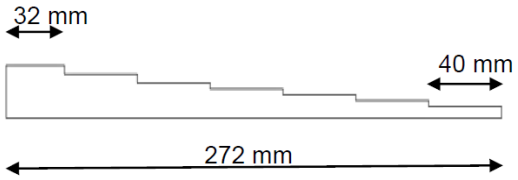

FIGURE 1. Step wedge description

The step wedge material composition is described in the following table.

TABLE 1. Chemical composition of the step wedge

Component	Specific percentage
Iron	97.038
Chromium	0.18
carbon	0.16
silicon	0.015
manganese	1.3
phosphorus	0.01
sulfur	0.007
Nickel	0.74
Molybdenum	0.48
Copper	0.06

The experimental set up is shown Fig 2. The source-cassette distance is 1000 mm. The step wedge is placed in contact with the cassette. The lead stopping screen is placed under the cassette. The source is adjusted with a plumb line in the center of the step wedge.

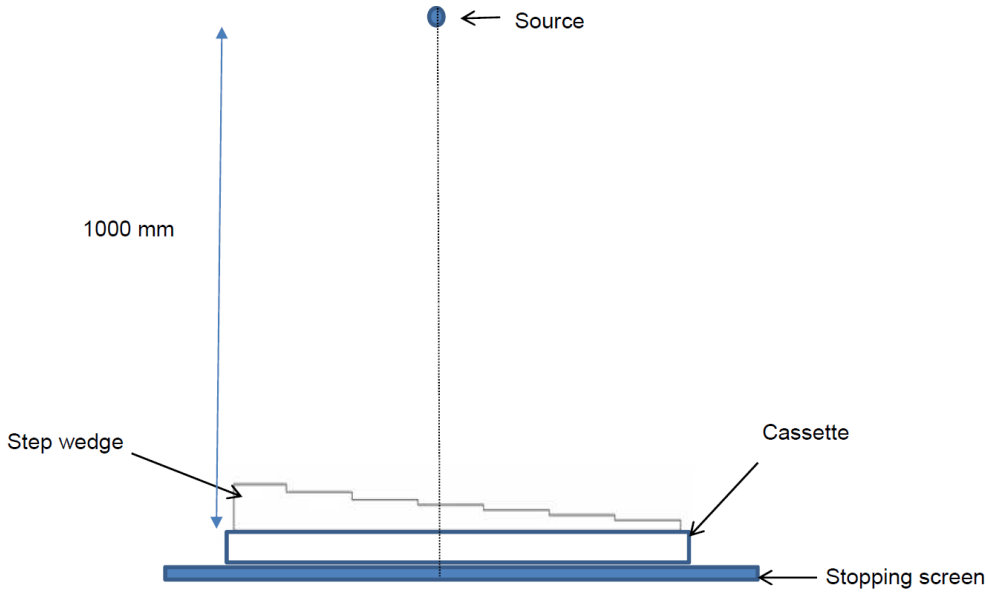

FIGURE 2. Benchmark setup

Ir192 and Se75 gamma sources used are cylinder-shaped with a diameter of 3 mm and a length of 3 mm. The cassette composition is:

- Front filter 0.5 mm Pb (10 cm x 40 cm)
- Reinforced screen 0.2 mm Pb (10 cm x 40 cm)
- M100 or AA400 X-ray film (10 cm x 40 cm), HR or GP image plate (10 cm x 48 cm),

The stopping lead screen is 3 mm thick.

X-ray films or image plates are placed in contact with the reinforced screen. The image plates KODAK HR and GP are read by a DURR NDT CR35 HR device, with a pitch of 50 µm for HR and 100 µm for GP. The X-ray films KODAK M100 and AA400 are developed manually at 20 °C and scanned with an AGFA FS50B device with a pitch of 50 µm. The following table presents a synthesis of the experimental parameters.

TABLE 2. Synthesis of the experimental parameters

Detector type	Source	Activity in Ci	Exposure time	Pixel size
Kodak HR	Ir192	19.32	1H50	50 µm
Kodak GP	Ir192	19.14	24 min	100 µm
Kodak HR	Se75	28.6	3H	50 µm
Kodak GP	Se75	28.77	38 min	100 µm
Kodak M100	Ir192	17.26	1H56	50 µm
Kodak M100	Se75	24.9	4H45	50 µm
Kodak AA400	Ir192	16.78	27 min	50 µm
Kodak AA400	Se75	26.38	59 min	50 µm

In CIVA [2], radiographic film modelling is based on the European standard EN 584 [3] and described in [4]. For the film characterization, an optical density (D) versus dose (k) curve is plotted for the entire range of optical densities between 1 and 4.5 (see fig. 3). Based on the EN584-1 standard three characteristic values ks, G2 and G4 are extracted from these measurements and only these three values are generally published in manufacturer certificates (X-ray tube 220 kV).

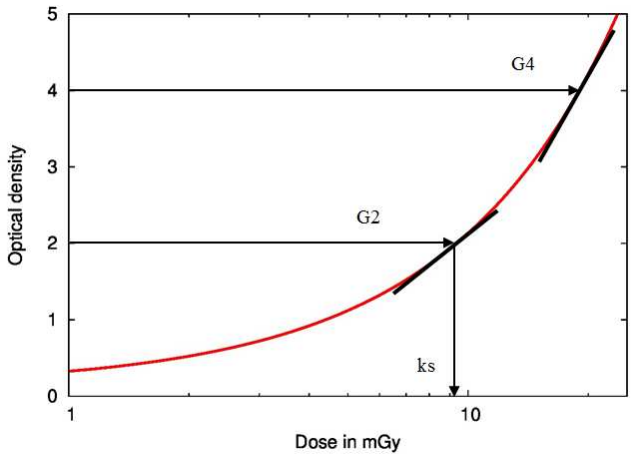

FIGURE 3. Optical density versus dose curve

D(k) can be approximated with a second order model using k_s and G2 values:

$$D(k) = Do + \frac{2}{k_s}k + ck^2 \qquad \text{a)}$$

Where

$$c = \frac{G2\log e - 2}{2{k_s}^2} \qquad \text{b)}$$

D_0 denotes the measured optical density of an unexposed film and includes fog and base density.
The granularity noise is approximated with a Gaussian distribution based on the granularity value (σ_D) available in manufacturers' certificates,

$$\sigma''_D = \sigma_D \sqrt{\frac{\pi * 10000}{4A}} \sqrt{\frac{D}{2}} \qquad \text{c)}$$

Where A is the pixel surface in µm².

Image plates modelling is based on the Monte-Carlo code Penelope [5], which simulates the response of an imaging plate in terms of deposited energy for a given incident radiation beam. In this model, a certain number of assumptions are necessary to model the imaging plate stack with the substrate material, the active phosphor layer and the protective layer, both in terms of thickness and in terms of material composition, as shown schematically in fig. 4.

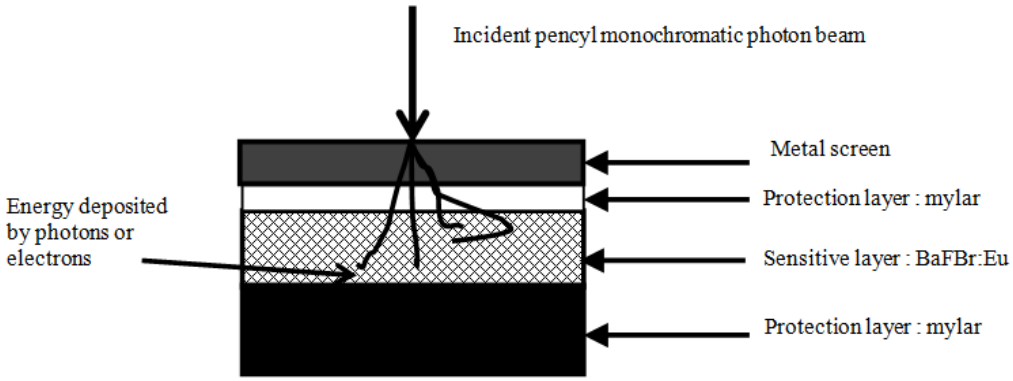

FIGURE 4. Penelope setup modeling [6]

The actual detector response corresponds to the energy deposited in the phosphorus layer. An hypothesis of a linear relationship between the deposited energy and the gray level is made which in fact is an approximation. By scanning the entire energy range, it is possible to obtain the spectral response (or quantum efficiency) of the imaging plate. While it is not computationally feasible to use a code like Penelope to calculate an entire radiographic inspection, it is possible to use the spectral response to determine equivalent absorption coefficients, which can then be used in an engineering model to take into account the spectral detector response [6] (see fig 5).

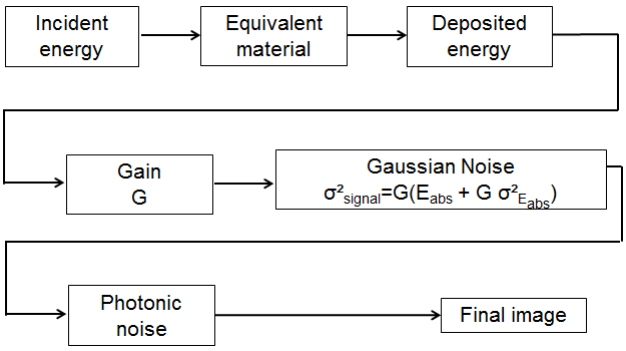

FIGURE 5. Image plate modelling setup in CIVA

CIVA RESULTS

For this benchmark, we have performed a qualitative and quantitative comparison with real data. For the qualitative comparison, we extract a linear intensity profile along the axis of the step wedge from experimental and simulated images. The line profile thickness is 1 pixel (see fig. 6) and the size of the simulated image is the same as the size of the real detector.

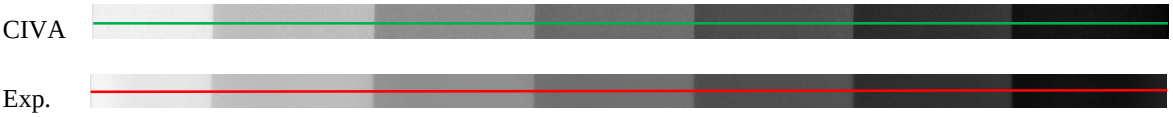

FIGURE 6. Example of experimental and simulated images with line profile extraction. For better clarity, we display a crop of both images along the considered profile.

For each acquisition configuration (source – detector), the optical density profile extracted from the simulated image is superimposed on the profile of the corresponding experimental image (see fig. 7).

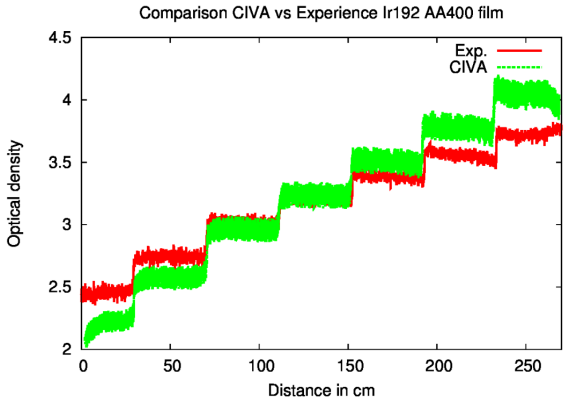

FIGURE 7. Example of intensity line profile comparison between CIVA and experimental data for an Ir192 gamma source and AA400 X-ray film.

Fig. 8 presents all the line profiles comparison obtained with AA400 and M100 X-ray film.

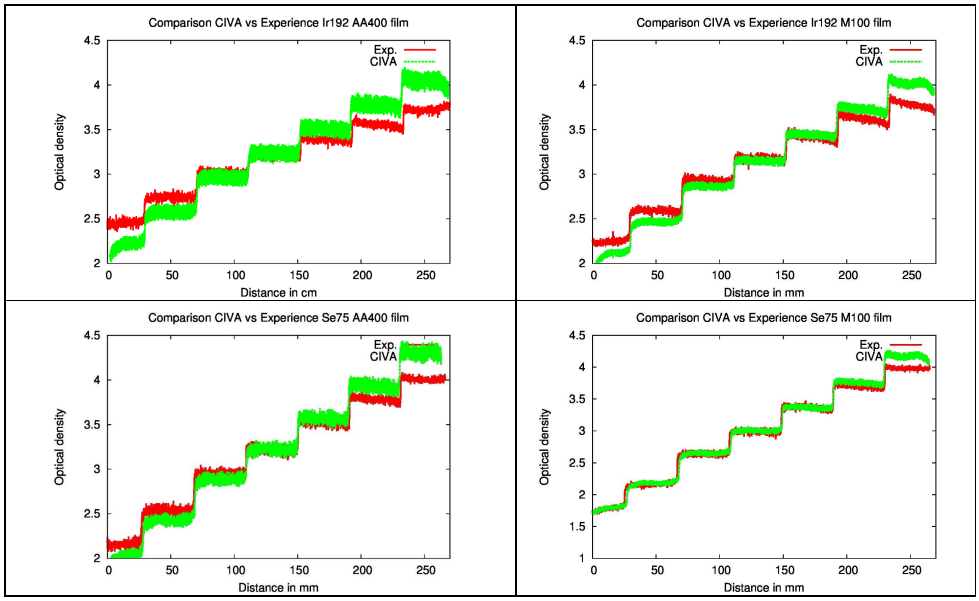

FIGURE 8 Intensity line profiles comparison between CIVA and experimental data for an Ir192 and Se75 gamma source and AA400 and M100 X-ray film.

Fig. 9 presents all the line profile comparison obtained with GP and HR image plate.

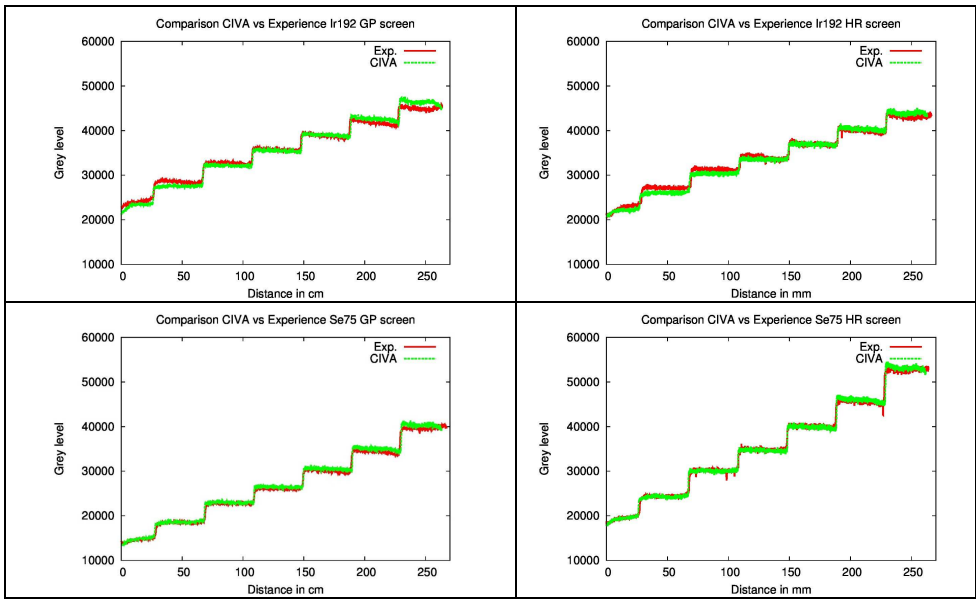

FIGURE 9 Intensity line profile comparison between CIVA and experimental data for an Ir192 and Se75 gamma source and GP and HR image plate.

For the quantitative comparison, we have computed the mean value and standard deviation in a 50 pixels by 50 pixels region of interest taken in the middle of each step. The following tables present the results synthesis: μ represents the mean value, σ represents the standard deviation, MSEμ represents the mean square deviation on the mean and MSEσ represents the mean square deviation on the standard deviation.

TABLE 3. Synthesis of the comparison between CIVA and experimental data with AA400 and M100 X-ray film with an Ir192 gamma source

Step thickness	exp		civa		MSE μ	MSE σ	exp		civa		MSE μ	MSE σ
mm	μ	2σ/μ	μ	2σ/μ			μ	2σ/μ	μ	2σ/μ		
18	2.45	2.9%	2.24	4.0%	8.6%	40.6%	2.24	1.7%	2.12	2.2%	5.3%	27.9%
15	2.75	2.8%	2.58	3.7%	6.1%	28.3%	2.58	1.8%	2.47	1.9%	4.6%	9.3%
12	3.03	2.6%	2.96	3.5%	2.1%	32.8%	2.93	1.8%	2.87	1.9%	1.9%	5.9%
10	3.21	2.4%	3.23	3.3%	0.8%	38.4%	3.16	1.6%	3.15	1.8%	0.4%	8.1%
8	3.38	2.1%	3.51	3.2%	3.8%	49.9%	3.42	1.4%	3.44	1.7%	0.6%	20.0%
6	3.55	1.9%	3.78	3.1%	6.4%	60.4%	3.63	1.2%	3.73	1.6%	2.8%	32.6%
4	3.70	1.6%	4.04	3.0%	9.2%	92.6%	3.77	1.1%	4.02	1.6%	6.6%	43.0%
	Ir192, AA400				5.3%	49.0%	**Ir192, M100**				3.18%	21.0%

TABLE 4. Synthesis of the comparison between CIVA and experimental data with AA400 and M100 X-ray film with a Se75 gamma source

Step thickness	exp		civa		MSE μ	MSE σ	exp		civa		MSE μ	MSE σ
mm	μ	2σ/μ	μ	2σ/μ			μ	2σ/μ	μ	2σ/μ		
18	2.2	3.1%	2.0	4.1%	6.0%	31.4%	1.76	2.0%	1.79	2.5%	1.53%	20.4%
15	2.6	3.1%	2.4	3.9%	4.6%	26.3%	2.14	2.1%	2.18	2.2%	1.91%	7.0%
12	3.0	2.8%	2.9	3.5%	2.3%	24.3%	2.62	2.0%	2.64	2.0%	0.92%	0.9%
10	3.2	2.4%	3.2	3.3%	0.5%	36.6%	2.97	2.0%	3.00	1.9%	0.98%	4.4%
8	3.5	2.0%	3.6	3.1%	0.7%	54.5%	3.36	1.6%	3.37	1.7%	0.36%	7.0%
6	3.8	1.5%	3.9	3.0%	3.1%	104.4%	3.71	1.2%	3.76	1.6%	1.24%	39.2%
4	4.0	1.1%	4.3	2.9%	7.0%	163.4%	4.01	0.9%	4.17	1.6%	4.17%	66.7%
	Se75, AA400				3.5%	63.0%	**Se75, M100**				1.6%	20.8%

Fig. 8 and tables 3 and 4 show a good agreement between experimental optical density and CIVA simulation for AA400 and M100 X-ray films with a respective mean error MSEμ of 5.3% and 3.2% for Ir192, 3.5% and 1.6% for Se75. Simulations with Se75 are more accurate to experimental data than Ir192 simulations. This is due to the fact that the X-ray film modelling is based on 220 kV X-ray spectrum and Se75 gamma source has a lower spectrum than Ir192. However the noise simulated in CIVA seems to be overestimated. The noise average overestimation is 49% for AA400 and 21% for M100. The origin of this discrepancy has been identified in the code and corresponds to a “bug” which will be corrected for CIVA next version.

TABLE 5. Synthesis of the comparison between CIVA and experimental data with GP and HR image plate with an Ir192 gamma source

Step thickness	**exp**		**civa**		**MSE μ**	**MSE σ**	**exp**		**civa**		**MSE μ**	**MSE σ**
mm	**μ**	**2σ/μ**	**μ**	**2σ/μ**			**μ**	**2σ/μ**	**μ**	**2σ/μ**		
18	24034	1.6%	22607	1.8%	5.9%	12.5%	22808	1.9%	22195	2.0%	2.7%	3.2%
15	28578	1.4%	26908	1.6%	5.8%	14.2%	27140	1.8%	26037	1.9%	4.1%	1.7%
12	32914	1.4%	31484	1.5%	4.3%	2.8%	31200	1.6%	30391	1.7%	2.6%	3.5%
10	35732	1.3%	34805	1.4%	2.6%	2.2%	34029	1.6%	33596	1.6%	1.3%	3.2%
8	38738	1.4%	38266	1.3%	1.2%	5.4%	37413	1.5%	36921	1.6%	1.3%	2.8%
6	41587	1.4%	41842	1.2%	0.6%	8.1%	40392	1.5%	40301	1.5%	0.2%	3.3%
4	44726	1.4%	45664	1.2%	2.1%	13.3%	43269	1.5%	43750	1.4%	1.1%	3.3%
	Ir192, GP				3.2%	8.4%	**Ir192, HR**				1.9%	3.0%

TABLE 6. Synthesis of the comparison between CIVA and experimental data with GP and HR image plate with a Se75 gamma

Step thickness	**exp**		**civa**		**MSE μ**	**MSE σ**	**exp**		**civa**		**MSE μ**	**MSE σ**
mm	**μ**	**2σ/μ**	**μ**	**2σ/μ**			**μ**	**2σ/μ**	**μ**	**2σ/μ**		
18	14663	1.7%	14782	2.0%	0.8%	13.3%	19671	2.0%	19338	2.1%	1.7%	2.2%
15	18499	1.6%	18584	1.7%	0.5%	6.5%	24535	1.8%	24232	1.9%	1.2%	3.1%
12	22751	1.5%	22970	1.5%	1.0%	0.2%	30234	1.7%	30098	1.7%	0.4%	3.4%
10	26156	1.4%	26442	1.4%	1.1%	1.1%	34874	1.7%	34716	1.6%	0.5%	6.4%
8	30069	1.3%	30449	1.3%	1.3%	4.2%	40169	1.6%	39952	1.4%	0.5%	8.5%
6	34487	1.3%	34969	1.1%	1.4%	16.3%	45807	1.5%	45959	1.3%	0.3%	14.2%
4	39482	1.3%	40379	1.1%	2.3%	16.8%	52835	1.3%	53015	1.2%	0.3%	7.7%
	Se75, GP				1.2%	8.3%	**Se75, HR**				0.7%	6.5%

Fig. 9 and tables 5 and 6 show a very good agreement between experimental optical density and CIVA simulation for GP and HR image plate with a respectively mean MSEμ of 3.2% and 3.0% for Ir192 and 1.2% and 0.7% for Se75. Noise simulated in CIVA is slightly overestimated. The noise average overestimation is 8.3% for GP and 4.8% for HR. These errors are compatible with our model hypothesis.

CONCLUSION

In this work we presented results from the World Federation of NDEC 2014 RT modelling benchmark with the RT models implemented in the CIVA software. These models concern X-ray films and image plates. After a short presentation of the benchmark and CIVA modelling approach, we described a comparison between simulation and experimental data. For X-ray films modelling, our comparisons demonstrated a good agreement in terms of optical density but a noise overestimation. This problem has been identified and it will be corrected in the next CIVA version. The comparison for image plates showed a very good agreement in terms of grey level and noise. This benchmark could be enriched with an unsharpness comparison. Further characterizations for other IP/screen combinations will be added and further validations using other sources and wall thicknesses are planned.

REFERENCES

1. http://www.wfndec.org/
2. http://www-civa.cea.fr
3. EN 584-1:2006, "Non-destructive testing – Industrial radiographic film – Part 1: Classification of film systems for industrial radiography", European standard for non-destructive evaluation
4. A. Schumm, U. Zscherpel, “The EN584 standard for the classification of industrial radiography films and its use in radiographic modelling”, in Proceedings of the Sixth International Conference on NDE in relation to structural integrity for nuclear and pressurized components (2007).
5. F. Salvat, J. M. Fernandez-Varea, J. Baro, J. Sempau, “PENELOPE, an algorithm and computer code for Monte Carlo simulation of electron-photon showers,” Informes Tecnicos Ciemat, 799, CIEMAT,Madrid, Spain (1996)
6. D. Tisseur, M. Costin, F. Mathy, A. Schumm, “Simulation of Computed radiography with Imaging Plate Detectors”, QNDE2013, AIP Conf. Proc. 1581, 1861 (2014)